Ziv-Zakai bound for rate-constrained time-delay estimation in a wireless sensor network

Sriram Srinivasan
Digital Signal Processing Group
Philips Research Laboratories
High Tech Campus 36, 5656AE Eindhoven, The Netherlands.
sriram.srinivasan@philips.com

Abstract – *Source localization is an important application of wireless sensor networks, and time-delay estimation is an essential step in several location finding algorithms. Various performance bounds for time-delay estimation have been developed for the case where the complete data from all individual sensors is considered available at the fusion center. In a wireless sensor network however, there exists a constraint on the number of bits that may be wirelessly exchanged between the sensors. This paper investigates performance bounds on time-delay estimation under a rate constraint, where the estimation is performed at the fusion center using signals that have been encoded with the available rate R. The Ziv-Zakai bound, which has been shown to subsume other bounds such as the Barankin and the Cramer-Rao bound as special cases, is obtained for the rate-constrained case and used to analyze the relation between the communication bit-rate and the variance of the time-delay estimation error.*

Keywords: Time-delay estimation, rate constraint, Ziv-Zakai bound.

1 Introduction

In source localization, signals received at two or more sensors are combined to obtain an estimate of the location of the sound source. Source localization has several applications, e.g., aeroacoustic tracking of ground vehicles in military applications, localization of underwater acoustic beacons, bio-medical applications such as ultrasonic imaging, self-localization of nodes in sensor networks, wildlife habitat monitoring etc. In the absence of signal-specific information, accurate localization can be accomplished by estimating the differential delay between pairs of sensor signals [1,2]. Time-delay (TD) estimation is usually performed using the generalized cross-correlation approach [3,4].

This paper deals with the TD estimation problem in distributed sensor networks where the different sensors are connected wirelessly, and there exists a constraint on the number of bits that may be exchanged between the sensors. Such a constraint is relevant as wireless transmission is more power intensive than other processing steps, e.g., to compress the signal to transmit as few bits as possible [5]. The effect of a finite bit-rate on the resulting TD estimation error thus merits further study. It is assumed that the communication between a node and the fusion center is limited to R bits per second. The focus is on studying the relation between the bit-rate R and the resulting accuracy of TD estimation. This can be done by expressing a lower bound on the variance of the estimation error as a function of the bit-rate.

Quantizers designed specifically for the TD estimation task have been studied in [6,7]. Such quantizers typically require knowledge of e.g., the joint probability distribution of the sensor signals. In this paper, TD estimation is considered in the absence of any prior information. Furthermore, it is assumed that the sensor signals received at the fusion center are used not only for TD estimation but also for other tasks such as signal estimation through beamforming. Thus, in the absence of prior information, and in this general setting, the sensors simply encode their signals so as to minimize the mean-squared signal reconstruction error, and TD estimation is performed at the fusion center using the encoded signals.

In the absence of rate constraints, performance bounds on the mean-square TD estimation error have been extensively studied [8–13]. A commonly used bound is the Cramér-Rao lower bound (CRLB) [3], a natural choice given that it is asymptotically attained by a maximum-likelihood estimator. For TD estimation using narrowband signals however, the CRLB is tight only for exceedingly high signal-to-noise ratios (SNRs) or large observation times [14]. In the rate constrained case, this limitation of the CRLB becomes significant when analyzing performance at low bit-rates. Several approaches have been formulated to address this limitation, e.g., using the Chapman-Robbins version of the Barankin bound [14], and the improved Ziv-Zakai bound (ZZB) [9–11,15]. The ZZB is more general, has been found to be tighter than the Barankin bound [9], and incorporates the CRLB as a limiting case.

In this paper, using results from classical rate-distortion theory, the ZZB on the mean-square TD estimation error is

derived for the case where the sensors transmit their signals at a rate R to the fusion center. The ZZB in [9, 10] depends on the fractional bandwidth, the SNR, and the time-bandwidth product. In the rate-constrained case considered in this paper, in addition to the above parameters, the ZZB depends on the bit-rate R as well, and this relation is explored by varying R for fixed values of the fractional bandwidth, the SNR, and the time-bandwidth product. An expression for the minimum bit-rate at the which the ZZB converges to the CRLB is also derived.

2 Signal model

The discussion in this paper is limited to the case of two microphones. The following signal model holds for the TD estimation problem:

$$\begin{aligned} x_1(t) &= s(t) + n_1(t) \\ x_2(t) &= s(t - \Delta\tau) + n_2(t), \quad -T/2 \le t \le T/2, \end{aligned} \tag{1}$$

where $x_1(t)$ and $x_2(t)$ are the received microphone signals, $s(t)$ is the source signal, $\Delta\tau$ is the differential time-delay, $n_1(t)$ and $n_2(t)$ are the noise processes at the two sensors, and T is the observation time. The signals $s(t)$, $n_1(t)$, and $n_2(t)$ are assumed to be zero-mean stationary mutually independent Gaussian random processes with power spectral densities $\Phi_s(\omega)$, $\Phi_{n_1}(\omega)$, and $\Phi_{n_2}(\omega)$, respectively.

It is assumed that each node encodes its signal at a rate R before transmission to the fusion center, where the TD estimate is obtained from the two signals. This situation is depicted in Fig. 1. Scenarios where one of the nodes is the fusion center can then be treated as special cases where the rate corresponding to that node is infinity. Note that the signal model in (1) incorporates the presence of acoustic noise, but the channel will be assumed to be lossless to study the impact of encoding the source signals at a rate R on TD estimation.

When a signal $x(t)$ is encoded at a rate R, the relation between R and the resulting reconstruction error can be expressed by the following parametric rate-distortion relation [16]:

$$\begin{aligned} R(\lambda) &= \frac{1}{4\pi}\int_{-\infty}^{\infty} \max\left(0, \log_2 \frac{\Phi_x(\omega)}{\lambda}\right) d\omega, \\ D(\lambda) &= \frac{1}{2\pi}\int_{-\infty}^{\infty} \min(\lambda, \Phi_x(\omega)) d\omega, \end{aligned} \tag{2}$$

where $\Phi_x(\omega)$ is the PSD of $x(t)$. The distortion here is the mean-squared error (MSE) between $x(t)$ and its reconstruction. Equation (2) provides the relation between the number of bits R used to represent the signal, and the resulting distortion D in the reconstructed signal. As the relation between R and D cannot be obtained in closed form, it is expressed in terms of a parameter λ. Inserting a particular value of λ in (2) results in certain rate R, and a corresponding distortion D. An R-D curve is obtained as λ traverses

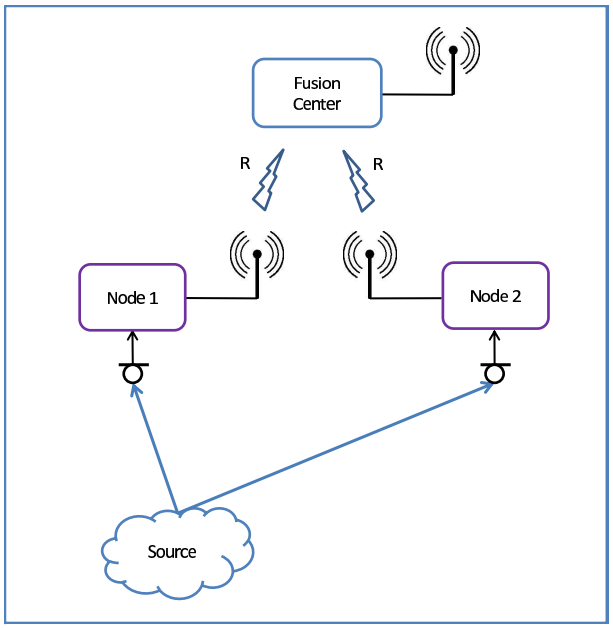

Figure 1: Each node transmits its observed signal at a rate R to the fusion center where the TD estimate is obtained.

the interval $[0, \text{ess sup } \Phi_x(\omega)]$, where ess sup is the essential supremum.

Let $x_1^{R_1}(t)$ and $x_2^{R_2}(t)$ denote the signals transmitted by the two nodes, at rates R_1 and R_2, respectively. It is assumed that the channel is lossless. The TD estimate is obtained using signals $x_1^{R_1}(t)$ and $x_2^{R_2}(t)$ at the fusion center. The signal $x_1^{R_1}(t)$ is depicted in Fig. 2 using the *forward channel* representation [16]. It is obtained by first bandlimiting $x_1(n)$ with a filter with frequency response

$$B_1(\omega) = \max\left(0, \frac{\Phi_{x_1}(\omega) - \lambda_1}{\Phi_{x_1}(\omega)}\right), \tag{3}$$

and then adding independent zero-mean (non-white) Gaussian noise with PSD given by

$$\Phi_{z_1}(\omega) = \max\left(0, \lambda_1 \frac{\Phi_{x_1}(\omega) - \lambda_1}{\Phi_{x_1}(\omega)}\right). \tag{4}$$

Note that both $B_1(\omega)$ and $\Phi_{z_1}(\omega)$ are real-valued. A similar forward channel representation holds for the signal $x_2(n)$ with $B_2(\omega)$ and $\Phi_{z_2}(\omega)$ defined analogously.

3 Ziv-Zakai lower bound for rate-constrained TD estimation

To obtain the ZZB on the variance of the TD estimation error, the TD $\Delta\tau$ is assumed to be a random variable uniformly distributed in an interval $[-D/2, D/2]$. Let $\bar{\epsilon^2}$ denote the mean-square estimation error. A general expression for the ZZB is given by [9]

$$\bar{\epsilon^2} \ge \frac{1}{D}\int_0^D xG[(D-x)P_e(x)]dx, \tag{5}$$

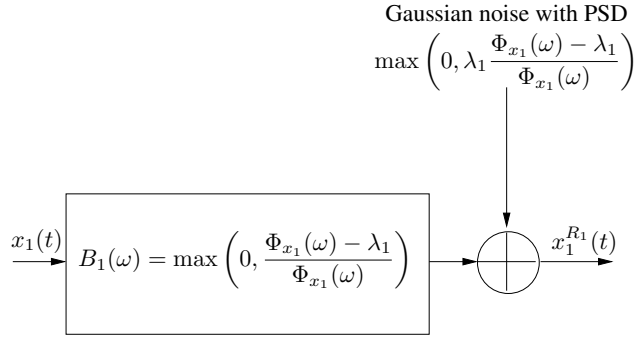

Figure 2: The forward channel representation.

where $P_e(x)$ is the minimum attainable probability of error associated with the likelihood ratio test for determining whether the true TD value is $\Delta\tau_0$ or $\Delta\tau_1$ with $x = \Delta\tau_1 - \Delta\tau_0$. $G[\cdot]$ is a non-increasing function of x obtained by filling the valleys of the function $(D-x)P_e(x)$. Assuming that the observation time is large compared to the correlation time $2\pi/W$, where W is the signal bandwidth, adapting the steps in [9] to the rate-constrained case, it can be shown that $P_e(x)$ is given by

$$P_e(x) = e^{a(x)+b(x)}\phi(\sqrt{2b(x)}) \tag{6}$$

where

$$a(x) = -\frac{T}{2\pi}\int_0^\infty \ln[1+\gamma(\omega,x)]d\omega, \tag{7}$$

$$b(x) = \frac{T}{2\pi}\int_0^\infty \frac{\gamma(\omega,x)}{1+\gamma(\omega,x)}d\omega, \tag{8}$$

$$\gamma(\omega,x) = \xi(\omega,R_1,R_2)\sin^2(\omega x/2), \tag{9}$$

$$\xi(\omega,R_1,R_2) = \frac{\frac{B_1^2(\omega)\Phi_s(\omega)}{B_1^2(\omega)\Phi_{n_1}(\omega)+\Phi_{z_1}(\omega)}\frac{B_2^2(\omega)\Phi_s(\omega)}{B_2^2(\omega)\Phi_{n_2}(\omega)+\Phi_{z_2}(\omega)}}{1+\frac{B_1^2(\omega)\Phi_s(\omega)}{B_1^2(\omega)\Phi_{n_1}(\omega)+\Phi_{z_1}(\omega)}+\frac{B_2^2(\omega)\Phi_s(\omega)}{B_2^2(\omega)\Phi_{n_2}(\omega)+\Phi_{z_2}(\omega)}}, \tag{10}$$

and

$$\phi(y) = \frac{1}{\sqrt{2\pi}}\int_y^\infty e^{-\frac{t^2}{2}}dt. \tag{11}$$

The unconstrained case becomes a special case of the above solution where setting $R_1 = R_2 = \infty$ in (10) results in $B_1(\omega) = B_2(\omega) = 1$, and $\Phi_{z_1}(\omega) = \Phi_{z_2}(\omega) = 0$, so that

$$\xi(\omega,R_1,R_2)_{|R_1=R_2=\infty} = \frac{\frac{\Phi_s(\omega)}{\Phi_{n_1}(\omega)}\frac{\Phi_s(\omega)}{\Phi_{n_2}(\omega)}}{1+\frac{\Phi_s(\omega)}{\Phi_{n_2}(\omega)}+\frac{\Phi_s(\omega)}{\Phi_{n_1}(\omega)}}, \tag{12}$$

which is identical to the result obtained in [9, eqs. 19-23].

For general signal and noise PSDs, the ZZB can be obtained from (5) by numerical integration. If the signal and noise PSDs are assumed to be flat in a band W rad/s around a center frequency ω_0 rad/s, and zero otherwise, then the closed-form expressions derived in [10] can be applied. Let

$$\Phi_s(\omega) = \begin{cases}\Phi_s & |\omega_0-\omega| \le W/2,\\ 0 & |\omega_0-\omega| > W/2\end{cases} \tag{13}$$

and for $i = 1, 2$,

$$\Phi_{n_i}(\omega) = \begin{cases}\Phi_{n_i} & |\omega_0-\omega| \le W/2,\\ 0 & |\omega_0-\omega| > W/2.\end{cases} \tag{14}$$

Consequently, $\xi(\omega, R_1, R_2)$ in (10) becomes independent of frequency, and will be denoted $\xi(R_1, R_2)$ in the following. The term $\xi(R_1, R_2)$ is referred to in TD estimation literature as the SNR, due to the SNR like appearance of the expression in (12), and the term $(WT/2\pi)\xi(R_1, R_2)$ is referred to as the post-integration SNR. Under the assumptions that $W/\omega_0 \ll 1$ (small fractional bandwidth), and $\omega_0 D \gg 2\pi$ (the correlation time is lower than the maximum expected delay), the ZZB becomes [9]

$$\bar{\epsilon^2} \ge \begin{cases} D^2/12 & \frac{WT}{2\pi}\xi(R_1,R_2) \le \xi_1\\ \frac{6}{W^2}\frac{1}{(WT/2\pi)\xi(R_1,R_2)} & \xi_1 < \frac{WT}{2\pi}\xi(R_1,R_2) \le \xi_2\\ \text{Thresholdregion} & \xi_2 < \frac{WT}{2\pi}\xi(R_1,R_2) \le \xi_3\\ \frac{1}{2\omega_0^2}\frac{1}{(WT/2\pi)\xi(R_1,R_2)} & \frac{WT}{2\pi}\xi(R_1,R_2) > \xi_3, \end{cases} \tag{15}$$

where

$$\begin{aligned}\xi_1 &= \frac{72}{WT/2\pi}\left(\frac{\omega_0}{W}\right)^2\left(\frac{1}{WD}\right)^2\\ \xi_2 &= \frac{2.17}{\pi^2 WT/2\pi}\left(\frac{\omega_0}{W}\right)^2\\ \xi_3 &= \frac{6}{\pi^2}\left(\frac{\omega_0}{W}\right)^2\left[\phi^{-1}\left(\frac{W^2}{24\omega_0^2}\right)\right]^2.\end{aligned} \tag{16}$$

The first row of (15) corresponds to the case where the measurements are dominated by noise and do not contribute to the TD estimation. In this case, the error is bounded by the available prior information. The second row of (15) is the Barankin bound, and the final row is the CRLB. The ZZB varies exponentially with the post-integration SNR in the threshold region. ξ_1 corresponds to the post-integration SNR at which the ZZB is 3 dB below $D^2/12$, which is the bound determined by prior knowledge about the range of expected delay values. ξ_2 and ξ_3 correspond to the post-integration SNRs at which the ZZB is 3 dB above the third and fifth lines of (15), respectively.

Fig. 3 plots the ZZB, normalized by the a-priori bound $D^2/12$, for different values of the post-integration SNR, obtained through numerical integration of (5) using the approximations in [9, eq. 62]. As in [9], the relevant parameter values are set to $W/\omega_0 = 0.1$ ($W = 2\pi\ 20$, $\omega_0 = 2\pi\ 200$),

$WT/2\pi = 64$, and $\omega_0 D/2\pi = 11$, so that the required assumptions are satisfied. The SNR thresholds predicted by (16) are depicted by the dotted lines, and match the behavior of the ZZB well.

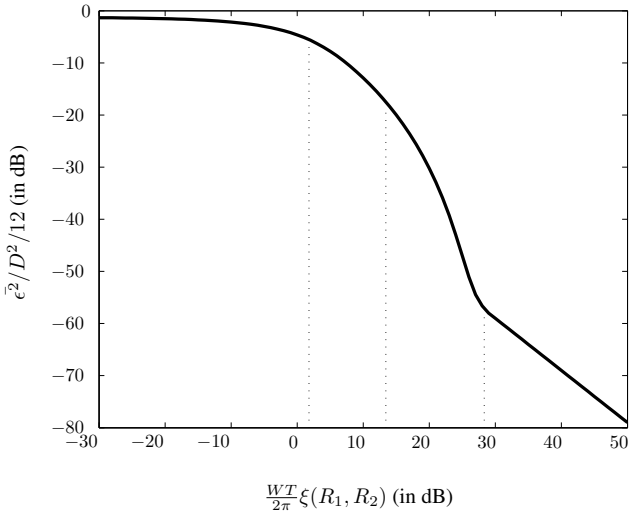

Figure 3: ZZB as a function of the post-integration SNR, for a source signal with fractional bandwidth $W/\omega_0 = 0.1$, $WT/2\pi = 64$, and $\omega_0 D/2\pi = 11$. The dotted lines indicate the thresholds predicted by (16).

The bounds ξ_1 and ξ_3 are of particular interest in the rate constrained case. The bit-rate at which $\xi(R_1, R_2) = \frac{2\pi\xi_1}{WT}$ corresponds to the minimum rate at which wireless transmission starts to become useful. Below this rate, the error is bounded by the prior information. The bit-rate at which $\xi(R_1, R_2) = \frac{2\pi\xi_4}{WT}$ corresponds to the minimum rate at which the CRLB is tight. Under the assumption that $R_1 = R_2 = R$, the relation between R and a given value $\xi^\star$ of the SNR $\xi(R_1, R_2)$ is derived in the following section, which can then be used to analyze various aspects of the ZZB in relation to the bit-rate.

4 Expressing the ZZB in terms of the bit-rate

Fig. 3 plots the ZZB in terms of $\xi(R_1, R_2)$, which is defined in (10). To obtain the ZZB directly in terms of the bit-rate, the quantity $\xi(R_1, R_2)$ needs to be explicitly expressed in terms of the bit-rate.

Let $R_1 = R_2 = R$, $\Phi_{n_1} = \Phi_{n_2} = \Phi_n$, and $\Phi_x = \Phi_s + \Phi_n$. Then $\Phi_{x_1} = \Phi_{x_2} = \Phi_x$, $\Phi_{z_1} = \Phi_{z_2} = \Phi_z$, and $B_1 = B_2 = B$. Denote $\xi(R_1, R_2) = \xi(R)$. For the signal model (13) and (14), using (2)-(4), one obtains

$$B = 1 - 2^{-2\pi R/W}, \tag{17}$$

and

$$\Phi_z = B\Phi_x 2^{-2\pi R/W}. \tag{18}$$

Employing the above assumptions in (10), $\xi(R)$ becomes

$$\xi(R) = \frac{B^4\Phi_s^2}{(B^2\Phi_n + \Phi_z)^2 + 2B^2\Phi_s(B^2\Phi_n + \Phi_z)}. \tag{19}$$

Inserting (17) and (18) into (19) and re-arranging the terms yields

$$\xi(R) = \frac{\Phi_s^2}{\Phi_n^2 + 2\Phi_s\Phi_n + 2\Phi_x^2\beta + \Phi_x^2\beta^2}, \tag{20}$$

where

$$\beta = \frac{2^{-2\pi R/W}}{1 - 2^{-2\pi R/W}}. \tag{21}$$

Equation (20) can be expressed as a quadratic in β. Discarding the negative solution results in

$$\frac{2^{-2\pi R/W}}{1 - 2^{-2\pi R/W}} = \frac{\rho}{1+\rho}\sqrt{\frac{1+\xi(R)}{\xi(R)}} - 1, \tag{22}$$

where $\rho = \Phi_s/\Phi_n$. Re-arranging the terms in (22) yields

$$\xi(R) = \frac{1}{(1+\beta)^2\left(\frac{\rho+1}{\rho}\right)^2 - 1} \tag{23}$$

Equivalently, for a given ρ and bandwidth W, the rate R that results is a value $\xi^\star$ of $\xi(R)$ can also be obtained from (22), and is given by

$$R(\xi^\star) = \frac{W}{2\pi}\log_2\left(\frac{\eta}{\eta - 1}\right), \tag{24}$$

where

$$\eta = \frac{\rho}{1+\rho}\sqrt{\frac{1+\xi^\star}{\xi^\star}}. \tag{25}$$

Thus $R(\frac{2\pi\xi_1}{WT})$ is the minimum bit-rate in bits per second (bps) at which the ZZB is 3 dB lower than the a-priori bound $\mathcal{D}^2/12$. If the available bit-rate is lower than $R(\frac{2\pi\xi_1}{WT})$, then transmission is redundant. Similarly, $R(\frac{2\pi\xi_4}{WT})$ is the minimum bit-rate at which the CRLB is attained.

Employing the same parameters used to generate Fig. 3, the normalized ZZB (solid) obtained through direct evaluation of (5) is plotted as a function of bit-rate in Fig. 4, with $\rho = 10^4$. For these values of the fractional bandwidth, time-bandwidth product, and ρ, it can be seen that a minimum bit-rate of approx. 5 bps is required for transmission to be meaningful. Below this rate, the the a-priori bound is valid. The dashed line represents the CRLB, given by the last row of the approximation (15). As expected, the ZZB and the CRLB coincide at high bit- rates, the threshold in this case being around 90 bits per second. Below this threshold however, it is evident that the ZZB represents a tighter bound than the CRLB. Finally, it can be seen from Fig. 4 that performance saturates at a bit-rate of around 300 bps. For the signal parameters in this example, a higher bit-rate does not lower the bound.

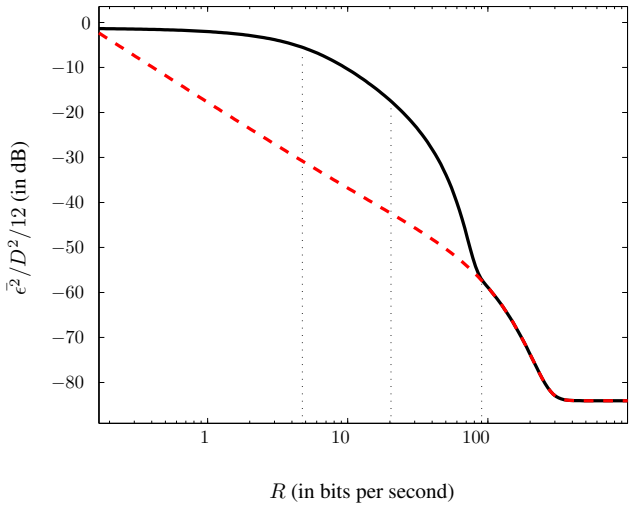

Figure 4: ZZB (solid) as a function of the bit-rate R, for a source signal with fractional bandwidth $W/\omega_0 = 0.1$, $WT/2\pi = 64$, and $\omega_0 D/2\pi = 11$. The CRLB (dashed), given by the last line of (15) is also shown. While the two bounds match at high bit-rate, the ZZB is tighter at lower bit-rates.

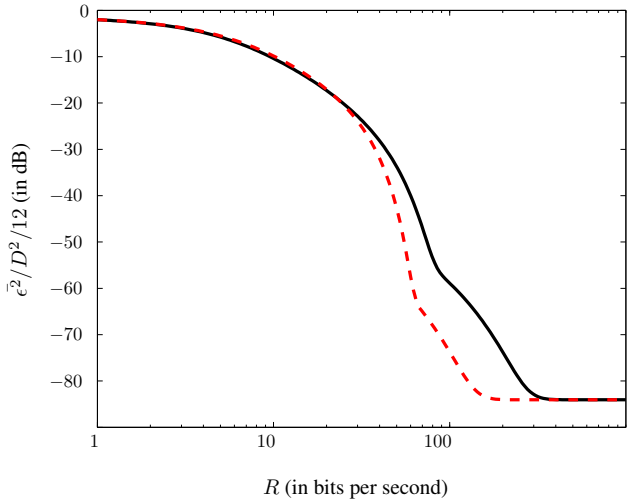

Figure 5: ZZB as a function of the bit-rate R, for two different bandwidths $W_1 = 2\pi\ 20$ (solid), and $W_2 = 2\pi\ 10$ (dashed). For both cases, the time bandwidth product is the same, $W_i T/2\pi = 64$ for $i = 1, 2$, and $\omega_0 D/2\pi = 11$. In the range $30 \leq R \leq 300$, the lower bandwidth W_2 provides better performance.

Fig. 5 plots the ZZB as a function of the bit-rate for two different bandwidths, $W_1 = 2\pi\ 20$ (solid), and $W_2 = 2\pi\ 10$ (dashed). In both cases, the time bandwidth product is the same, $W_i T/2\pi = 64$ for $i = 1, 2$, and $\omega_0 D/2\pi = 11$. While it is well known that higher bandwidths provide better TD estimates, the behavior in the rate-constrained case is different. When the bit-rate is between approx. 30 and 300 bps, it can be seen from Fig. 5 that a lower bandwidth results in a lower bound for the error. The loss due to the lower bandwidth is more than offset by the longer observation interval, and as transmitting a signal with a higher bandwidth requires more bits, one observes the behavior seen in Fig. 5.

The CRLB in the case without rate constraints depends only on the time bandwidth product. In the rate-constrained case however, the term $\xi(R_1, R_2)$ in the expression for the CRLB (last line of (15)) also depends on the bandwidth, as can be seen from (23) and (21). Hence the difference in behavior in the CRLB region (rate above approx. 60 bps) in Fig. 5. Beyond a certain threshold bit-rate, which is approx. 350 bps in this example, the savings in bit-rate resulting from having to transmit a lower bandwidth signal disappear and the two curves coincide[1].

When the time bandwidth product is not constant, the behavior of the ZZB over R differs from that observed in Fig. 5 as the bandwidth is varied. Fig. 6 plots the the ZZB over R for bandwidths $W_1 = 2\pi\ 20$ (solid) and $W_2 = 2\pi\ 10$ (dashed), and $\omega_0 D/2\pi = 11$. The observation duration however is fixed to satisfy $W_1 T/2\pi = 64$, resulting in a shorter duration for the smaller bandwidth case. At low bit-rates (below approx. 60 bps), W_1 provides better performance as the system can be expected to benefit from the higher time-bandwidth product in the presence of a significant amount of quantization noise. At medium bit-rates (between 60 and approx. 200 bps) W_2 provides better performance as fewer bits are needed to describe the signal. At high bit-rates the higher bandwidth W_1, which in this case also implies a higher time bandwidth product, provides better performance and is consistent with the behavior observed in the traditional unconstrained case.

[1] It is to be noted that this behavior also depends on the value of ρ.

5 Conclusions

The Ziv-Zakai bound on the variance of the time-delay estimation error has been obtained for the rate-constrained scenario, where the nodes in a wireless sensor network transmit their signals at a rate R to the fusion center. The individual nodes encode their signals using the given rate R so as to minimize the mean-squared reconstruction error, and time-delay estimation is performed at the fusion center using the compressed signals.

For a given signal center frequency, bandwidth, observation length and SNR, the relation between the bound and the bit-rate obtained in this paper can be used to specify the bit-rate required to achieve a desired level of estimation accuracy. The relation can also be used to determine relevant parameters such as the minimum rate at which transmission becomes meaningful, i.e., the resulting error variance is less than the a-priori bound, and the rate at which the Cramer-Rao bound is tight.

Besides establishing the relation between the bound and the bit-rate, the analysis also reveals some useful interesting findings specific to the rate-constrained case. E.g., within a certain range of bit-rate values, which depends on the signal parameters, a lower bandwidth signal results in a lower

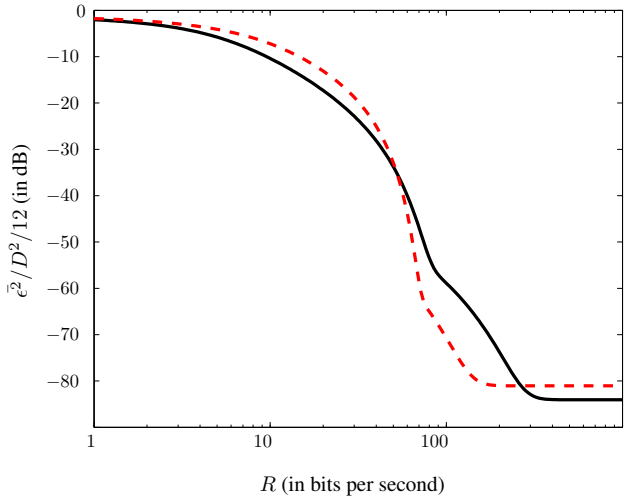

Figure 6: ZZB as a function of the bit-rate R, for two different bandwidths such that $W_1/\omega_0 = 0.1$ (solid), $W_2/\omega_0 = 0.05$ (dashed), and $\omega_0 D/2\pi = 11$. The observation duration is fixed such that $W_1 T/2\pi = 64$, resulting in different time bandwidth products.

bound for the variance of the estimation error than a higher bandwidth signal, whereas in the traditional wired set-up a higher bandwidth always results in better performance. This can be intuitively explained by the fact that more bits are needed to describe a higher bandwidth signal, while not all the signal information is relevant to the time-delay estimation task. As the bit-rate increases beyond a certain threshold, the behavior is consistent with that observed in the unconstrained case.

References

[1] K. Yao, R. E. Hudson, C. W. Reed, D. Chen, and F. Lorenzelli, "Blind beamforming on a randomly distributed sensor array system," *IEEE Journal on Selected Areas in Communication*, vol. 16, no. 8, pp. 1555 –1567, Oct. 1998.

[2] T. Ajdler, I. Kozintsev, R. Lienhart, and M. Vetterli, "Acoustic source localization in distributed sensor networks," in *Thirty-Eighth Asilomar Conference on Signals, Systems and Computers*, vol. 2, Nov. 2004, pp. 1328 – 1332 Vol.2.

[3] C. Knapp and G. Carter, "The generalized correlation method for estimation of time delay," *IEEE Trans. Acoustics, Speech, Signal Processing*, vol. 24, no. 4, pp. 320–327, Aug. 1976.

[4] G. Carter, "Coherence and time delay estimation," *Proceedings of the IEEE*, vol. 75, no. 2, pp. 236–255, Feb. 1987.

[5] G. J. Pottie and W. J. Kaiser, "Wireless integrated network sensors," *Commun. ACM*, vol. 43, no. 5, pp. 51–58, 2000.

[6] M. Chen and M. L. Fowler, "Optimizing non-MSE distortion for data compression in emitter location systems," in *2003 Conference on Information Sciences and Systems*, Mar. 2003, pp. 243–254.

[7] L. Vasudevan, A. Ortega, and U. Mitra, "Application-specific compression for time delay estimation in sensor networks," in *1st International conference on Embedded networked sensor systems (SenSys '03)*, 2003, pp. 243–254.

[8] A. Weiss and E. Weinstein, "Composite bound on the attainable mean square error in passive time-delay estimation from ambiguity prone signals (corresp.)," *IEEE Trans. Inform. Theory*, vol. 28, no. 6, pp. 977 – 979, Nov. 1982.

[9] ——, "Fundamental limitations in passive time delay estimation–Part I: Narrow-band systems," *IEEE Trans. Acoustics, Speech, Signal Processing*, vol. 31, no. 2, pp. 472–486, Apr. 1983.

[10] E. Weinstein and A. Weiss, "Fundamental limitations in passive time-delay estimation–Part II: Wide-band systems," *IEEE Trans. Acoustics, Speech, Signal Processing*, vol. 32, no. 5, pp. 1064–1078, Oct. 1984.

[11] J. Ianniello, E. Weinstein, and A. Weiss, "Comparison of the Ziv-Zakai lower bound on time delay estimation with correlator performance," in *Proc. IEEE Int. Conf. Acoustics, Speech, Signal Processing*, vol. 8, Apr. 1983, pp. 875 – 878.

[12] K. Scarbrough, R. Tremblay, and G. C. Carter, "Performance predictions for coherent and incoherent processing techniques of time delay estimation," *IEEE Trans. Acoustics, Speech, Signal Processing*, vol. 31, no. 5, pp. 1191 – 1196, Oct. 1983.

[13] B. Sadler and R. Kozick, "A survey of time delay estimation performance bounds," in *4th IEEE Workshop on Sensor Array and Multichannel Processing*, Jul. 2006, pp. 282–288.

[14] S.-K. Chow and P. Schultheiss, "Delay estimation using narrow-band processes," *IEEE Trans. Acoustics, Speech, Signal Processing*, vol. 29, no. 3, pp. 478–484, Jun. 1981.

[15] B. M. Sadler, N. Liu, and Z. Xu, "Ziv-Zakai bound on time delay estimation in unknown convolutive random channels," in *5th IEEE Sensor Array and Multichannel Signal Processing Workshop*, Jul. 2008, pp. 390 –394.

[16] T. Berger, *Rate distortion theory: a mathematical basis for data compression*, ser. Information and System Sciences Series, T. Kailath, Ed. Prentice Hall, 1971.